Growing Microtubules Push the Oocyte Nucleus to Polarize the *Drosophila* Dorsal-Ventral Axis

Tongtong Zhao *et al.*

Science **336**, 999 (2012);
DOI: 10.1126/science.1219147

Growing Microtubules Push the Oocyte Nucleus to Polarize the *Drosophila* Dorsal-Ventral Axis

Tongtong Zhao,[1] Owen S. Graham,[2] Alexandre Raposo,[1]* Daniel St Johnston[1]†

The *Drosophila* dorsal-ventral (DV) axis is polarized when the oocyte nucleus migrates from the posterior to the anterior margin of the oocyte. Prior work suggested that dynein pulls the nucleus to the anterior side along a polarized microtubule cytoskeleton, but this mechanism has not been tested. By imaging live oocytes, we find that the nucleus migrates with a posterior indentation that correlates with its direction of movement. Furthermore, both nuclear movement and the indentation depend on microtubule polymerization from centrosomes behind the nucleus. Thus, the nucleus is not pulled to the anterior but is pushed by the force exerted by growing microtubules. Nuclear migration and DV axis formation therefore depend on centrosome positioning early in oogenesis and are independent of anterior-posterior axis formation.

The correct positioning of the nucleus is important for several developmental processes, such as cell migration, formation of the neuromuscular junction, and asymmetric cell divisions, whereas nuclear mislocalization is a feature of neurological disorders, such as lissencephaly (*1*). Positioning of the nucleus plays an essential role in *Drosophila* axis formation, because the movement of the nucleus from the posterior of the oocyte to a point at its anterior circumference breaks radial symmetry to polarize the dorsal-ventral (DV) axis (*2*, *3*). At stage 7 of oogenesis, an unknown signal from the posterior follicle cells induces a major reorganization of the oocyte microtubule cytoskeleton. The posterior microtubule organizing center (MTOC) is disassembled, and microtubules are nucleated from the anterior-lateral cortex, resulting in an anterior-posterior (AP) gradient of microtubules that defines the AP axis (*4*). It is believed that dynein subsequently uses this polarized microtubule cytoskeleton to pull the nucleus to the oocyte anterior, making polarization of the DV axis dependent on the prior polarization of the AP axis (*5*–*9*).

The nucleus is pushed to the anterior by growing microtubules. To investigate the mechanism

[1]The Gurdon Institute and the Department of Genetics, University of Cambridge, Tennis Court Road, Cambridge CB2 1QN, UK. [2]The Department of Engineering, University of Cambridge, Trumpington Street, Cambridge CB2 1PZ, UK.

*Present address: Instituto Gulbenkian de Ciência, Rua da Quinta Grande, 6, P-2780-156 Oeiras, Portugal.
†To whom correspondence should be addressed. E-mail: d.stjohnston@gurdon.cam.ac.uk

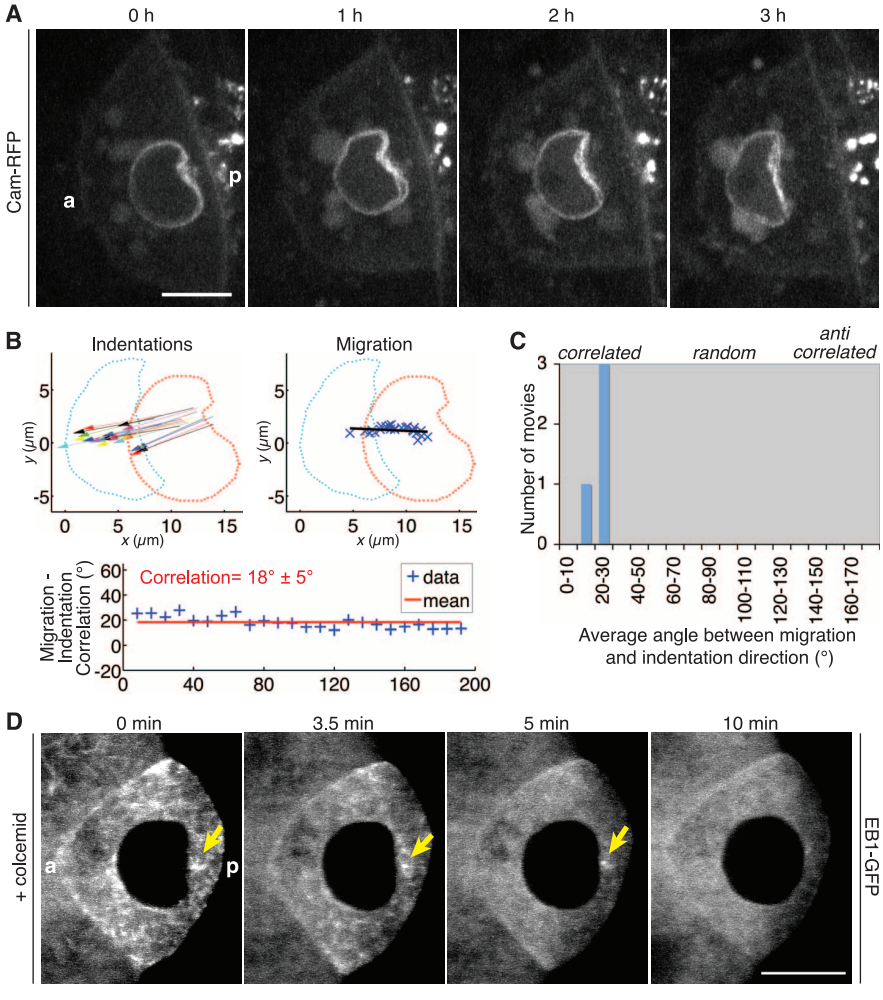

Fig. 1. Nuclear migration is driven by a posterior microtubule pushing force. (**A**) Time course of a migrating nucleus. RFP indicates red fluorescent protein. (**B**) Analysis of directions of nuclear indentations during migration (left), direction of overall migration (right), and the correlation between them, expressed as the angle between the directional vectors (bottom) (mean ± SD). Red and cyan dots show the outline of the nucleus at the start and end of migration, respectively; blue ×s show the centroid of the nucleus during migration. (**C**) Mean angle between migration and indentation directions from four migrating nuclei. (**D**) Temporal merges of an EB1-GFP movie of a colcemid-treated egg chamber. Each image is a maximum projection of five time frames (equal to 10 s). Arrow, MTOC. In (A) and (D), a, anterior; p, posterior; scale bars, 10 μm.

of nuclear positioning directly, we imaged the movement of the nucleus in living oocytes. The nucleus migrates at a speed of 4.0 ± 0.7 μm/hour (n = 6) and takes 2 to 3 hours to move across the oocyte (Fig. 1). The trajectory of the nucleus is variable: Sometimes it moves around the cortex of the oocyte directly to an anterior corner, but it often migrates up the center of the oocyte and then turns to move along the anterior cortex (fig. S1 and movie S1), confirming the random nature of this symmetry-breaking event. We observed that all migrating nuclei have large posterior indentations, suggesting that they are being pushed rather than pulled toward the anterior (Fig. 1A and movie S2). This could reflect an intrinsic reorganization of the nuclear architecture or a deformation induced by an external force to the nucleus. In support of the latter view, the direction of the indentation correlates with the direction of migration, suggesting that the same force creates the indentation and moves the nucleus (Fig. 1, B and C). This indentation is not an artifact of long-term imaging in oil, because egg chambers dissected directly into strong fixative have identical indentations (fig. S2).

This idea that the nucleus is pulled to the anterior by dynein has its basis in the finding that mutations in the dynein accessory factors, *Lis1* and *Bic-D*, as well as disruption of the dynactin complex result in mislocalized nuclei at stage 10 (*5*–*9*). This is not compatible with the pushing model of nuclear movement, because motor proteins can only pull their cargoes. We therefore reexamined the role of the dynein complex by imaging the nucleus in *Lis1* mutant egg chambers. *Lis1* mutant oocytes are much smaller than normal because dynein is required for transport from the nurse cells into the oocyte (*6*). Nevertheless, the oocyte nucleus migrates normally with a prominent posterior indentation (movie S3). Thus, dynein is presumably required for the anchoring of the nucleus once it has reached the anterior, rather than for its migration. Consistent with this, the nuclei are only rarely mispositioned in *Lis1* and *Bic-D* mutant oocytes at stage 9 but are mislocalized much more frequently at later stages (fig. S3).

Both actin and microtubule polymerization can generate pushing forces that lead to cellular or organelle deformations (*10*). Two lines of evidence suggest that microtubules are responsible for the nuclear indentation: First, depolymerization of actin with latrunculin A or B does not affect nuclear positioning, whereas the microtubule-depolymerizing drug colcemid induces mislocalized nuclei (*11*). Secondly, several microtubule-associated proteins become enriched on the posterior nuclear envelope during migration, including the dynein light intermediate chain (Dlic), calmodulin (Cam), and the *Drosophila* NuMA homolog mushroom body defect, Mud (fig. S4) (*12*–*14*).

To test the role of microtubules in the formation of the indentation, we added colcemid to living egg chambers expressing the +TIP protein, EB1-GFP (end binding-1–green fluorescent protein), which forms a "comet" on the growing plus ends of microtubules (*15*). Colcemid takes 3.5 min to diffuse into the oocyte, as monitored by a decrease in the number of EB1 comets on growing microtubule plus ends. As soon as microtubule growth starts to decrease, the indentation diminishes in size (Fig. 1D and movie S4). A focus of EB1-GFP persists posterior to the nucleus for several minutes, and, as this dis-

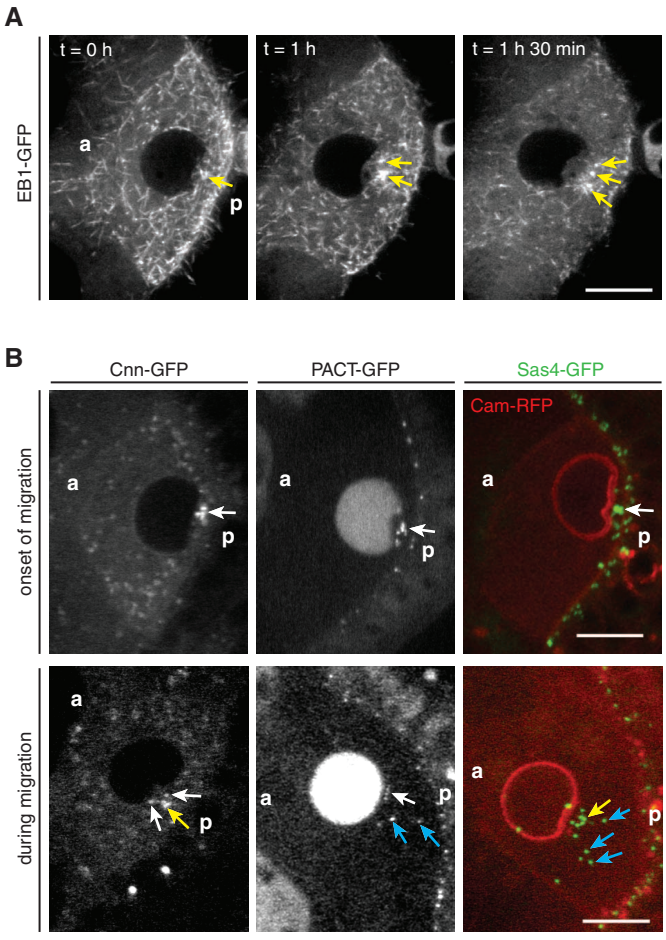

Fig. 2. Active centrosomes are localized behind the nuclear indentation. (**A**) Temporal merges (20 time frames, equal to 10 s) of an EB1-GFP movie reveal active MTOCs (arrows) between the nuclear indentation and the posterior oocyte cortex. (**B**) The centriolar markers PACT-GFP and Sas-4-GFP and the PCM marker Cnn-GFP are localized behind the nucleus at the onset of migration (top). During migration, MTOCs can be clustered together (yellow arrows), associated with the nucleus (white arrows), or dispersed in the cytoplasm (blue arrows) (bottom). Scale bars, 10 μm.

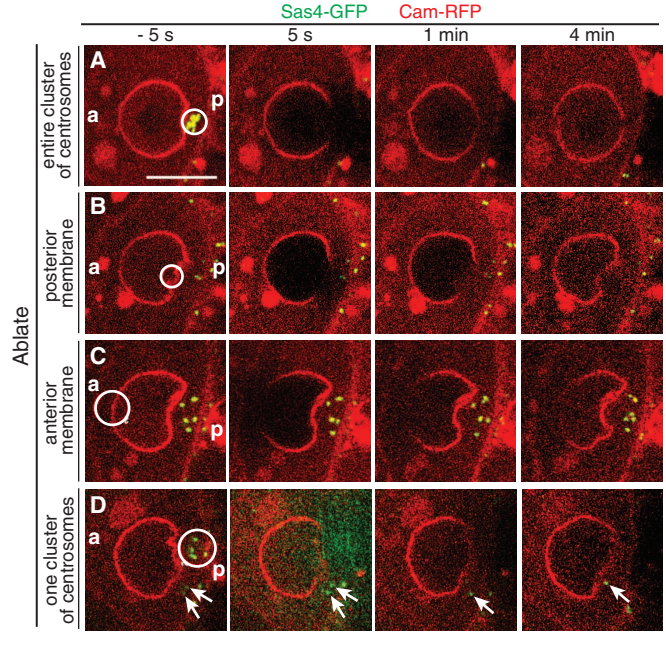

Fig. 3. Laser ablation of the centrosomes abolishes the nuclear indentation. (**A** and **D**) Clusters of centrosomes were bleached for 5 s. One to 4 min after ablation, the nuclear indentation facing the ablated centrosomes disappeared. (**B** and **C**) When the nuclear membrane or the anterior of the nucleus was bleached, the indentation was maintained. Circles, area of bleaching; arrows, nonablated, active centrosomes; scale bar, 10 μm.

appears, the nucleus relaxes completely and becomes spherical. Thus, the nuclear indentation depends on microtubule polymerization, and its size is proportional to the number of growing microtubules.

The nuclear indentation depends on active posterior centrosomes. Using EB1-GFP to track the growing microtubule plus ends in time-lapse movies of nuclear migration revealed several strong foci of EB1-GFP behind the indentation, with growing microtubules emanating from them in all directions (Fig. 2A and movie S5). This indicates that microtubules are nucleated from MTOCs behind the nucleus. These MTOCs resemble the centrosomes, which migrate from the nurse cells into the oocyte during early oogenesis in a dynein-dependent manner, and localize to the posterior cortex as a result of the initial oocyte polarity (*16*–*20*). Indeed, the centriolar markers Sas4 and PACT, as well as a marker for pericentriolar material (PCM), centrosomin (Cnn) (*21*), localize to the foci behind the nuclear indentation at the onset of migration (Fig. 2B). The centrosomes behave rather dynamically during migration and change reversibly from a dense cluster to a more dispersed distribution (Fig. 2B). Upon completion of nuclear migration, the centrosomes are recruited to the anterior-dorsal cortex of the oocyte, presumably as a consequence of the activation of the dynein-dependent anchoring mechanism that retains the nucleus in this position (fig. S5 and movies S6 and S7). Active centrosomes are therefore positioned behind the nucleus before and during migration.

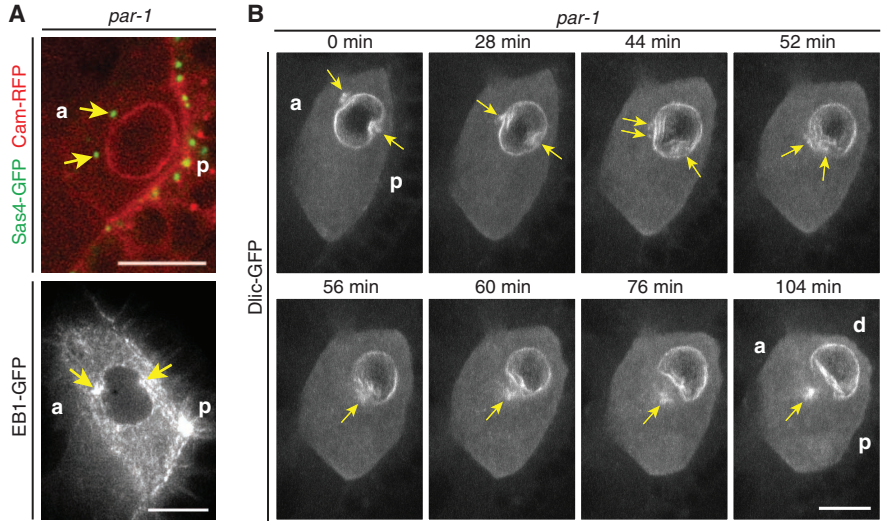

Fig. 4. Mispositioned centrosomes induce ectopic nuclear indentations. (**A**) Sas4-GFP (top) and a temporal merge of EB1-GFP (20 frames, equals 10 s) (bottom) reveal active, anterior centrosomes in *par-1*^{6323}/*par-1*^{W3} mutants, which induce an anterior indentation in the nucleus. (**B**) Nuclear migration in *par-1*^{6323}/*par-1*^{W3} mutants. At the onset of migration, the anterior centrosomes induce an ectopic anterior nuclear indentation. The anterior centrosomes eventually move around the nuclear membrane to cluster with the posterior centrosomes, inducing a broad nuclear indentation and rapid nuclear movement. d, dorsal; arrows, centrosomes; scale bars, 10 μm.

To test the role of the centrosomes in creating the nuclear indentation, we inactivated them by laser ablation. Upon ablation of the entire cluster of centrosomes, the indentation disappears, and the nucleus becomes spherical within 1 min (Fig. 3A and movie S8). This nuclear relaxation may occur more rapidly, because centrosome ablation causes local bleaching of the nuclear envelope, making it impossible to monitor nuclear shape during the first minute. However, local laser ablation of the nuclear envelope at the site of the indentation has no effect, excluding the possibility that the disappearance of the indentation is a consequence of bleaching of the nuclear membrane (Fig. 3B and movie S9). Furthermore, ablation of the anterior of the nucleus does not affect the indentation, arguing against any pulling force from the anterior (Fig. 3C and movie S10). As described above, centrosomes are sometimes scattered behind the nucleus, causing multiple indentations. Ablating one cluster of centrosomes abolishes only the indentation facing them. The nonablated centrosomes remain active and induce an indentation on the adjacent side of the nucleus (Fig. 3D and movie S11). Thus, the nucleus is not a rigid structure, and the growing microtubules from the centrosomes exert force on the nuclear envelope to induce its deformation.

The centrosomes are dispensable for oogenesis (*22*). We therefore examined nuclear migration in *DSas-4* mutant ovaries that lack centrosomes. Consistent with the previous study, all nuclei migrate to the anterior-dorsal corner ($n = 117$) and show a posterior indentation during migration (fig. S6 and movie S12). GFP-Cnn is still localized in foci behind the nucleus, and EB1-GFP tracks reveal active posterior MTOCs (fig. S6). Thus, acentrosomal MTOCs form in the absence of centrosomes and can provide the pushing force for nuclear migration.

Nuclear migration is independent of AP axis formation. As a further test of the idea that the centrosomal microtubules push the nucleus to the anterior, we examined *par-1* hypomorphs, in which some centrosomes fail to migrate to the posterior of the oocyte (*19*). These anterior

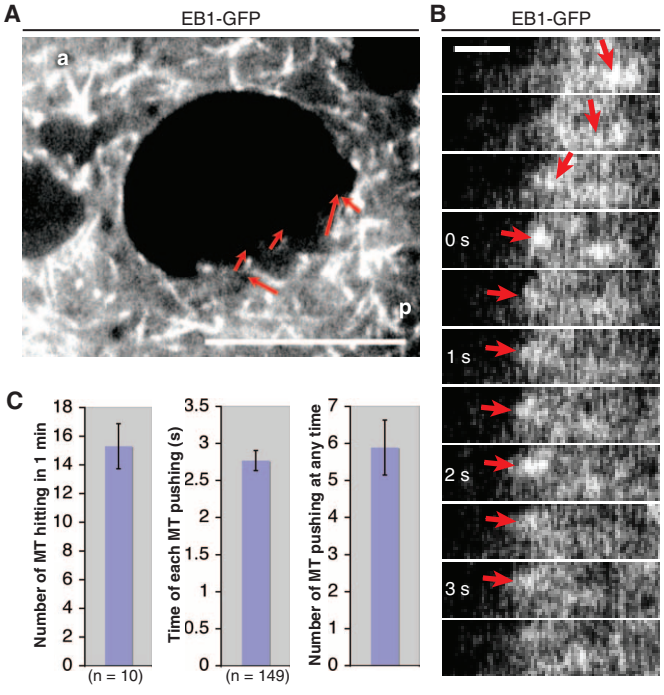

Fig. 5. The force of microtubule polymerization is sufficient to move the nucleus. Quantification of the number of microtubules hitting the posterior of the nucleus. (**A**) Temporal merge of 20 frames (equal to 10 s) of an EB1-GFP movie. Red arrows indicate tracked microtubules that hit the nuclear indentation. Scale bar, 10 μm. (**B**) Kymograph of a microtubule that pushes against the nuclear indentation for 3 s; arrows indicate the position of the EB1-GFP comet (plus end of a microtubule). Scale bar, 1 μm. (**C**) Quantification of the number of microtubules hitting the nuclear indentation, the time that each microtubule pushes, and the resulting average number of microtubules that are pushing against the indentation at any given time (error bars, ±SEM).

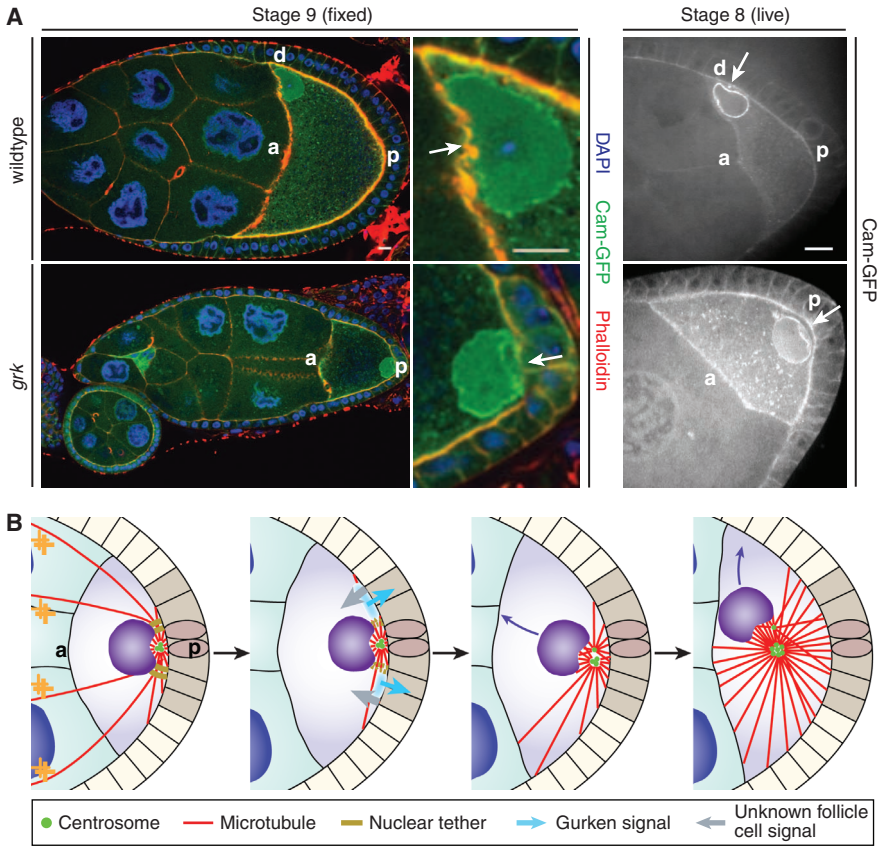

Fig. 6. The nucleus is anchored to the posterior before migration. (**A**) The nuclei often fail to migrate in *grk*^{2B6}/*grk2*^{E12} mutants but still have prominent posterior indentations (arrows), indicating that they are tethered at the posterior. DAPI, 4′,6-diamidino-2-phenylindole; scale bars, 10 μm. (**B**) A microtubule pushing model for nuclear migration. Before migration, the nucleus is tethered at the posterior with active centrosomes behind it (left). The posterior follicle cell signal induces the release of the nucleus from the tether, and growing microtubules then push the nucleus anteriorly (middle). This movement is essentially random and continues until the oocyte becomes wedged in an anterior corner (right).

centrosomes induce anterior nuclear indentations, leading to dumbbell-shaped nuclei, confirming the role of centrosomal microtubules in pushing the nucleus (Fig. 4A). These ectopic centrosomes eventually fuse with the posterior centrosomes to move the nucleus to the anterior-dorsal corner (Fig. 4B and movie S13). This explains why the nucleus migrates normally in *par-1* mutants even though the AP axis is not polarized (*23*). Consistent with this, the nucleus in wild-type oocytes can migrate to the anterior before the anterior-to-posterior microtubule gradient is established (Fig. 2A and fig. S7).

Microtubule growth provides sufficient force to move the nucleus. Another documented example of nuclear positioning by microtubule pushing comes from *Schizosaccharomyces pombe*, where microtubule bundles push against the cell ends to maintain the nucleus in the cell center (*24*). The oocyte nucleus moves a much greater distance, however, and appears to be pushed by the force exerted by single growing microtubules. To test the feasibility of this mechanism, we used Stoke's law ($F = 6\pi\eta r v$) to estimate the drag force (F) exerted on the nucleus. Assuming a cytoplasmic viscosity (η) ≈ 100 Pas (*25*, *26*) and the measured values of the nuclear radius (r) ≈ 5 μm and the velocity of migration (v) ≈ 4 μm/hour yields a drag force ≈ 10 pN. We expect the actual drag force to be lower, because nuclear migration is so slow (1 nm/s) that the cytoplasmic actin mesh will turn over ahead of the nucleus, decreasing the effective viscosity (*27*, *28*). The longest microtubules can reach ~10 μm between the posterior of the nucleus and the posterior oocyte cortex, resulting in a critical buckling force $F_c \approx 5$ pN (*29*). This value is probably an underestimate, because microtubules embedded within an elastic cytoplasm in vivo have been reported to bear compressive loads 100 times higher than those in vitro (*30*). Each microtubule can therefore generate a pushing force of at least 5 pN. Thus, the force of only two microtubules pushing at any time should be sufficient to move the nucleus to the oocyte anterior.

We measured the number of microtubules pushing the nucleus by using EB1-GFP. In one z plane, 15.3 ± 1.6 (SEM) microtubules hit the nuclear indentation per minute (n = 10, 2 oocytes), and they continued growing and presumably exerting force on the nucleus for 2.77 ± 0.14 s (n = 149) (Fig. 5, A to C, and movie S14). Given the thickness of a confocal section (0.8 μm) and the radius of the indentation [4.3 ± 0.2 μm (n = 10)], an average of 5.9 ± 0.7 microtubules were pushing the nucleus at any given time. Microtubule polymerization can therefore provide sufficient pushing force to drive nuclear migration.

Nuclear migration is triggered by release from a posterior anchor. The migration of the nucleus is triggered by an unknown signal from the posterior follicle cells, which could act either by activating the centrosomes or by releasing the nucleus from a posterior tether. To address this question, we examined when the indentation appears during oogenesis. Active centrosomes are already localized behind the nucleus at stage 5 of oogenesis and induce a posterior indentation (fig. S8A). This suggests that the centrosomes continually exert a pushing force on the nucleus, which is tethered to the posterior until it receives a signal for migration. The nucleus remains at the posterior in *gurken* (*grk*) mutants, which block follicle cell signaling to the oocyte (39% penetrance, n = 70) (*2*, *3*). These posterior nuclei still maintain a posterior indentation later in oogenesis (Fig. 6A), suggesting that they fail to migrate because they are not released from the posterior tether (fig. S8B and movie S15). Indeed, microtubules growing from active centrosomes probably always exert a pushing force on the nucleus that must be countered by an opposing pulling force or anchor to keep the nucleus in place. For example, a nuclear indentation is still visible adjacent to the centrosomes after the nucleus is anchored at the anterior (fig. S5A).

Our results lead to a revised model for how the oocyte nucleus moves to break radial symmetry and polarize the *Drosophila* DV axis (Fig. 6B). This model explains the failure to recover mutants that specifically disrupt nuclear migration, because the driving force is provided solely by microtubule polymerization. Furthermore, our results imply that migration is triggered by the release of the nucleus from a posterior anchor,

rather than by microtubule reorganization. Thus, polarization of the DV axis is independent of the formation of the microtubule array that defines the AP axis, as previously proposed.

References and Notes

1. I. Dupin, S. Etienne-Manneville, *Int. J. Biochem. Cell Biol.* **43**, 1698 (2011).
2. A. González-Reyes, H. Elliott, D. St Johnston, *Nature* **375**, 654 (1995).
3. S. Roth, F. S. Neuman-Silberberg, G. Barcelo, T. Schüpbach, *Cell* **81**, 967 (1995).
4. R. Bastock, D. St Johnston, *Curr. Biol.* **18**, R1082 (2008).
5. A. Swan, B. Suter, *Development* **122**, 3577 (1996).
6. A. Swan, T. Nguyen, B. Suter, *Nat. Cell Biol.* **1**, 444 (1999).
7. Y. Lei, R. Warrior, *Dev. Biol.* **226**, 57 (2000).
8. J. E. Duncan, R. Warrior, *Curr. Biol.* **12**, 1982 (2002).
9. J. Januschke *et al.*, *Curr. Biol.* **12**, 1971 (2002).
10. A. Mogilner, G. Oster, *Curr. Biol.* **13**, R721 (2003).
11. E. A. Koch, R. H. Spitzer, *Cell Tissue Res.* **228**, 21 (1983).
12. Y. C. Lee, J. Wolff, *J. Biol. Chem.* **257**, 6306 (1982).
13. J. R. Kardon, R. D. Vale, *Nat. Rev. Mol. Cell Biol.* **10**, 854 (2009).
14. A. E. Radulescu, D. W. Cleveland, *Trends Cell Biol.* **20**, 214 (2010).
15. Y. Mimori-Kiyosue, N. Shiina, S. Tsukita, *Curr. Biol.* **10**, 865 (2000).
16. A. P. Mahowald, J. M. Strassheim, *J. Cell Biol.* **45**, 306 (1970).
17. N. C. Grieder, M. de Cuevas, A. C. Spradling, *Development* **127**, 4253 (2000).
18. J. Bolívar *et al.*, *Development* **128**, 1889 (2001).
19. J. R. Huynh, J. M. Shulman, R. Benton, D. St Johnston, *Development* **128**, 1201 (2001).
20. P. Fichelson, M. Jagut, S. Lepanse, J. A. Lepesant, J. R. Huynh, *Development* **137**, 815 (2010).
21. N. M. Rusan, G. C. Rogers, *Traffic* **10**, 472 (2009).
22. N. R. Stevens, A. A. Raposo, R. Basto, D. St Johnston, J. W. Raff, *Curr. Biol.* **17**, 1498 (2007).
23. J. M. Shulman, R. Benton, D. St Johnston, *Cell* **101**, 377 (2000).
24. P. T. Tran, L. Marsh, V. Doye, S. Inoué, F. Chang, *J. Cell Biol.* **153**, 397 (2001).
25. A. R. Bausch, W. Möller, E. Sackmann, *Biophys. J.* **76**, 573 (1999).
26. R. M. Hochmuth, *J. Biomech.* **33**, 15 (2000).
27. K. Dahlgaard, A. A. Raposo, T. Niccoli, D. St Johnston, *Dev. Cell* **13**, 539 (2007).
28. N. Watanabe, *Proc. Jpn. Acad. Ser. B* **86**, 62 (2010).
29. M. Dogterom, J. W. Kerssemakers, G. Romet-Lemonne, M. E. Janson, *Curr. Opin. Cell Biol.* **17**, 67 (2005).
30. C. P. Brangwynne *et al.*, *J. Cell Biol.* **173**, 733 (2006).

Acknowledgments: We would like to thank J. Raff for providing the Dlic-GFP fly stock and centrosomal markers; H. Nash for providing the Mud antibody; S. Young for help with image analysis; and J. Guck, Y.-C. Oei, and P. K. Trong for help with the force calculations. This work was supported by a Wellcome Trust Principal Research Fellowship to D.St.J., Ph.D. scholarships from the FAZIT Stiftung, the Boehringer Ingelheim Fonds and the Cambridge European Trust to T.Z., the Gulbenkian Ph.D. scholarship of the Fundação para a Ciência e Tecnologia to A.R., and core support from the Wellcome Trust and Cancer Research UK.

Supplementary Materials

www.sciencemag.org/cgi/content/full/science.1219147/DC1
Materials and Methods
Figs. S1 to S8
References (*31*–*43*)
Movies S1 to S15

16 January 2012; accepted 27 March 2012
Published online 12 April 2012;
10.1126/science.1219147

Signatures of Majorana Fermions in Hybrid Superconductor-Semiconductor Nanowire Devices

V. Mourik,[1]* K. Zuo,[1]* S. M. Frolov,[1] S. R. Plissard,[2] E. P. A. M. Bakkers,[1,2] L. P. Kouwenhoven[1]†

Majorana fermions are particles identical to their own antiparticles. They have been theoretically predicted to exist in topological superconductors. Here, we report electrical measurements on indium antimonide nanowires contacted with one normal (gold) and one superconducting (niobium titanium nitride) electrode. Gate voltages vary electron density and define a tunnel barrier between normal and superconducting contacts. In the presence of magnetic fields on the order of 100 millitesla, we observe bound, midgap states at zero bias voltage. These bound states remain fixed to zero bias, even when magnetic fields and gate voltages are changed over considerable ranges. Our observations support the hypothesis of Majorana fermions in nanowires coupled to superconductors.

All elementary particles have an antiparticle of opposite charge (for example, an electron and a positron); the meeting of a particle with its antiparticle results in the annihilation of both. A special class of particles, called Majorana fermions, are predicted to exist that are identical to their own antiparticle (*1*). They may appear naturally as elementary particles or emerge as charge-neutral and zero-energy quasi-particles in a superconductor (*2*, *3*). Particularly interesting for the realization of qubits in quantum computing are pairs of localized Majoranas separated from each other by a superconducting region in a topological phase (*4*–*11*).

On the basis of earlier and later semiconductor-based proposals (*6*, *7*), Lutchyn *et al*. (*8*) and Oreg *et al*. (*9*) have outlined the necessary ingredients for engineering a nanowire device that should accommodate pairs of Majoranas. The starting point is a one-dimensional (1D) nanowire made of semiconducting material with strong spin-orbit interaction (Fig. 1A). In the presence of a magnetic field B along the axis of the nanowire (i.e., a Zeeman field), a gap is opened at the crossing between the two spin-orbit bands. If the Fermi energy μ is inside this gap, the degeneracy is twofold, whereas outside the gap it is fourfold. The next ingredient is to connect the semiconducting nanowire to an ordinary s-wave superconductor (Fig. 1A). The proximity of the superconductor induces pairing in the nanowire between electron states of opposite momentum and opposite spins and induces a gap, Δ. Combining this twofold degeneracy with an induced gap creates a topological superconductor (*4*–*11*). The condition for a topological phase is $E_Z > (\Delta^2 + \mu^2)^{1/2}$, with the Zeeman energy $E_Z = g\mu_B B/2$ (g is the Landé g factor, μ_B is the Bohr magneton). Near the ends of the wire, the electron density is reduced to zero, and subsequently, μ will drop below the subband energies such that μ^2 becomes large. At the points in space where $E_Z = (\Delta^2 + \mu^2)^{1/2}$, Majoranas arise as zero-energy (i.e., midgap) bound states—one at each end of the wire (*4*, *8*–*11*).

Despite their zero charge and energy, Majoranas can be detected in electrical measurements. Tunneling spectroscopy from a normal conductor into the end of the wire should reveal a state at zero energy (*12*–*14*). Here, we report the observation of such zero-energy peaks and show that they rigidly stick to zero energy while changing B and gate voltages over large ranges. Furthermore, we show that this zero-bias peak (ZBP) is absent if we take out any of the necessary ingredients of the Majorana proposals; that is, the rigid ZBP disappears for zero magnetic field, for a magnetic field parallel to the spin-orbit field, or when we take out the superconductivity.

[1]Kavli Institute of Nanoscience, Delft University of Technology, 2600 GA Delft, Netherlands. [2]Department of Applied Physics, Eindhoven University of Technology, 5600 MB Eindhoven, Netherlands.

*These authors contributed equally to this work.
†To whom correspondence should be addressed. E-mail: l.p.kouwenhoven@tudelft.nl